

Black hole accretion rings revealed by future X-ray spectroscopy

V. Sochora, V. Karas, J. Svoboda, and M. Dovčiak

Astronomical Institute, Academy of Sciences of the Czech Republic, Boční II 1401, CZ-141 31 Prague, Czech Republic

Accepted 2011 July 20; Received 2011 July 20; in original form 2011 January 25

ABSTRACT

Spectral features can arise by reflection of coronal X-rays on a black hole accretion disc. The resulting profile bears various imprints of strong gravitational field acting on the light emitting gas. The observed shape of the reflection line is formed by integrating contributions over a range of radii across the accretion disc plane, where the individual photons experience different level of energy shifts, boosting, and amplification by relativistic effects. These have to be convolved with the intrinsic emissivity of the line, which is a function of radius and the emission angle in the local frame. We study if the currently discussed instruments on-board X-ray satellites will be able to reveal the departure of the line radial emissivity from a simple smooth power-law function, which is often assumed in data fitting and interpretation. Such a departure can be a result of excess emission occurring at a certain distance. This could be used to study variations with radius of the line production or to constrain the position of the inner edge of the accretion disc. By simulating artificial data from a bright active galactic nucleus of a type-1 Seyfert galaxy (inclination $\simeq 30^\circ$, X-ray flux $\simeq 1\text{--}2$ mCrab in keV energy band) we show that the required sensitivity and energy resolution could be reached with Large Area Detector of the proposed LOFT mission. Galactic black holes will provide another category of potentially suitable targets if the relativistic spectral features are indeed produced by reflection from their accretion discs.

Key words: black hole physics — accretion, accretion disks — galaxies: nuclei

1 INTRODUCTION

Various pieces of evidence support the idea that the X-ray emission from active galactic nuclei (AGN; see Fabian et al. 2000; Reynolds & Nowak 2003) and stellar-mass black-holes (Miller et al. 2002; McClintock & Remillard 2006) originates from an accretion disc and the surrounding corona. These are thought to be situated near a central black hole, no more than a few tens gravitational radii from the event horizon, giving rise to the relativistic effects in 6–7 keV iron line complex and the underlying continuum. The standard scheme of accretion discs (Novikov & Thorne 1973; Page & Thorne 1974) captures the main properties of accreting black holes surprisingly well, nevertheless, the model omits some important aspects. In particular, the radial profile of the source intrinsic emissivity is represented by a smooth function (decaying as a power law $\propto r^{-3}$ at large distance), while the realistic profile is likely to be more complicated.

Different approaches have been pursued in order to understand how accretion disc X-ray spectra are formed. Generally, these include the investigations of accretion disc insta-

bilities as well as the interpretation of spectra to constrain the model parameters (such as the black hole spin, the source orientation, and the location and size of the accretion disc), and to determine the radial profile of accretion disc emissivity (Fabian et al. 2004). Recently, Wilkins & Fabian (2011) discussed an interesting approach to the inversion problem of determining the radial emissivity bulk profile of the relativistic broad iron line in Seyfert galaxy 1H 0707-495. Here we turn our attention to additional features superposed on top of the broad line.

The form of the inner accretion flow remains an open question. According to the standard scheme the flow proceeds down to the inner edge at the innermost stable circular orbit (ISCO), i.e., $r_{\text{ISCO}} = 6r_g$ for Schwarzschild black hole, and $r_{\text{ISCO}} = 1r_g$ for an extreme Kerr black hole (gravitational radius $r_g \equiv GM/c^2 \doteq 1.48 \times 10^{12} M_7$ cm with M_7 being the mass of the supermassive black hole in units of $10^7 M_\odot$). There are uncertainties about this assumption. It has been argued that because of magnetic stresses the radiation edge of the emission may be somewhat off the ISCO, and its exact location may be different for the continuum and for the iron line (Reynolds & Fabian 2008;

Abramowicz et al. 2010). Also, the inner rim recedes further out from the black hole when the accretion flow ceases and the disc becomes truncated, as was demonstrated in several objects (Markowitz et al. 2009; Svoboda et al. 2010, and references cited therein).

Intermittent episodes of a localized disc irradiation can naturally lead to a radially stratified emission profile rather than monotonic, continuous dependence of a standard accretion disc. We can approximate this configuration by radially constrained zones, which can be called “rings”. Let us remark that we are concerned with a spectral line emissivity, which is only partly related to the gas density; the essential quantity here is the ionization state of matter and how this varies with radius. Localized coronal irradiation of the disc material enhances the line emission above the mean value in the neighbourhood of a certain point. Integration of detected signal over a period of time then effectively produces a ring-type source (Goosmann et al. 2007).

In other words, one need not imagine physically separate rings and gaps emerging within the disc, even if this possibility has been also discussed; e.g. Cuadra et al. (2009) show a temporary density ring in an accretion disc surrounding a black-hole binary, while Artymowicz et al. (1993) and Karas & Šubr (2001) examine the process of gap formation by a secondary satellite embedded within the disc.

The excess emission from a certain radius could be revealed by high-resolution spectroscopy of the broad iron line (Karas & Sochora 2010), although at present it appears to be rather unfeasible because of insufficient signal-to-noise in the available data. In this paper we discuss whether the proposed Large Observatory for X-ray Timing (LOFT; Feroci et al. 2010, 2011) will have the necessary capability, at least for bright enough sources. To this end we produce artificial data with appropriate properties and then we analyze them by using a preliminary response file.

2 RECONSTRUCTING PARAMETERS FROM MODEL SPECTRUM

2.1 Local peaks of the broad line profile

According to the standard (stationary) accretion disc scenario, most radiation is produced within just a few gravitational radii above ISCO (up to $\simeq 20r_g$). Also various X-ray spectral features and the power-law component of the disc corona are believed to originate in that region. This main flux-producing area of the accretion disc is still rather wide in radius, hence it is thought to be the origin of the broad component of the line, which we include by employing the relativistic *kyrline* model (Dovčiak et al. 2004b).

Some reports suggest transient structures that are localized in radius and exhibit themselves as narrow features in the spectrum (e.g. Guainazzi 2003; Dovčiak et al. 2004a; de Marco et al. 2009, and references cited therein). In our picture of time-integrated spectra these are represented by rings. Although the significance of these features is still debated, their origin fits in the scenario of magnetic flares as sites of primary local illumination.

Magnetic flares are thought to occur above the accretion disc (Czerny et al. 2004; Uzdensky & Goodman 2008); in this context the line emission of the rings would arise not because the accretion disc develops such a physical structure,

but instead the localized emission by reconnection flares illuminates the underlying disc at a certain place, affecting there its ionization and producing the observable reflection features in spectrum. Rotation of the disc matter and time integration of the signal during observation produce belts out of point-like sites of illumination. In fact, we could then call these structures as reflection rings.

Although the mentioned scheme is our preferred way of effectively producing the rings, similar effects can arise by different mechanisms operating near a black hole. They can be broadly distinguished in two categories. Firstly, during the period of intermittent accretion the flow of material varies and the density profile and other variable (ionization state profile) can change along (e.g. King et al. 2006; Ballantyne et al. 2011). In another context, global spiral waves were suggested as a possible source of light curve modulation of accreting black holes (Tagger & Varnière 2006). Unlike ideal rings these spirals structures have a non-negligible radial extent, although to certain extent they could mimic rings in case of significant wounding in azimuthal direction (Karas et al. 2001). The formation of separate annuli occurs also in some models of strongly magnetized plasma discs (Coppi & Rousseau 2006). Finally, confined radii of enhance emission are a consequence of avalanche models (Pecháček et al., in preparation) where multiple flares arise in mutually connected families and gradually propagate towards the center before decaying at some characteristic distance.

In contrast to the model of major flares mentioned formerly, the latter alternatives appear to be unable of modulating the outgoing spectrum in any significant manner for a required period of time (Schnittman et al. 2006). Nonetheless, the current modelling has not yet provided a definitive answer and different options should be investigated further. In fact, the topic for debates is the expected level of the electromagnetic signal modulation above the noise and the ability to detect it by a given technology, rather than the existence of the modulation at a certain small level.

Aside from the mentioned speculations, one may ask if the actual presence of the rings can be tested. Here we thus presume that the structure develops and modulates the outgoing signal, and we want to verify whether the location of emission rings could be reconstructed from the observed spectrum. By *assuming the existence* of the modulation we investigate if these structures can be spectrally resolved in present-day or future X-ray spectra.

2.2 The method of calculation

To determine the relativistic shift (Doppler and gravitational) of the photon energy, we adopt the method described in our recent paper (Karas & Sochora 2010), where we considered propagation of photons from the source in the limit of geometrical optics in Kerr metric (Kato et al. 1998). The extremal values of energy shifts, g_{\max} and g_{\min} , are of particular interest, as they determine the range of line energy observed from distance. The main parameters are the emission radius $r = r_{\text{em}} \geq r_{\text{ISCO}}$, the dimensionless spin parameter a ($-1 \leq a \leq 1$), and the inclination angle i ($i = 0$ stands for the rotation axis, while $i = 90^\circ$ is for the edge-on view of the accretion disc). Extending our previous work, we allow also the case of retrograde rotation ($a < 0$) because such a

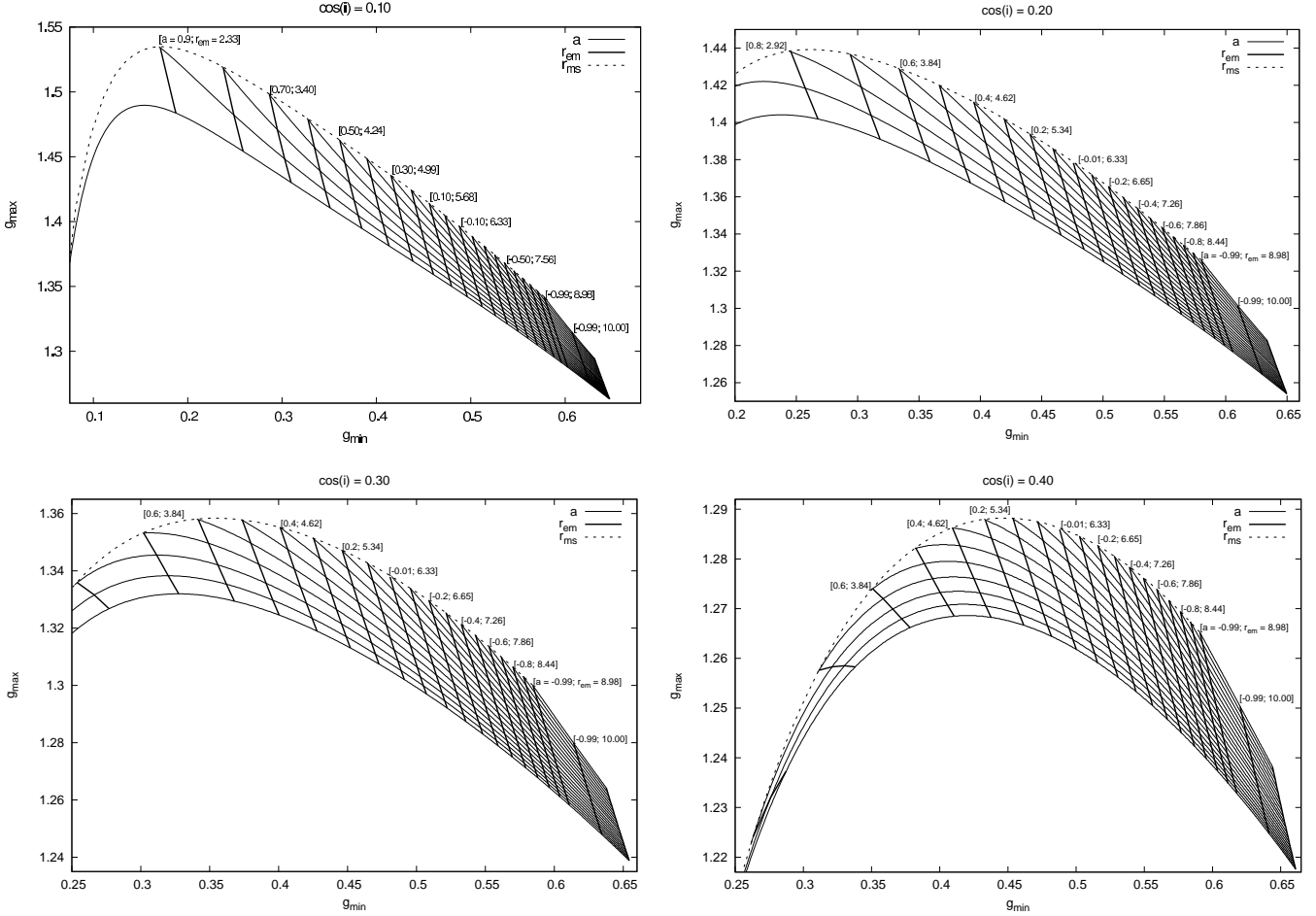


Figure 1. Observed energy of the line peaks, as determined by the extremal shifts g_{\max} versus g_{\min} for different view angles of the observer, $\cos i$. Each pair of g_{\max} , g_{\min} values corresponds to a certain emission radius, $r = r_{\text{em}}$, and the black hole spin a . Curves of constant emission radius r_{em} and the black hole spin a are shown (values are given in brackets). The ISCO radius coincides with the marginally stable orbit, $r = r_{\text{ms}}$, and it defines one boundary of the plot (dotted curve).

possibility is not excluded a priori, and it may lead naturally to rings that emerge at somewhat larger radii than in the prograde case (the ISCO recedes as counter-rotation of the black hole accelerates toward $a = -1$; Dauser et al. 2010).¹

A simple prescription for the intrinsic emission of light allows us to explore the observed spectral features across the parameter space. We assume a power-law continuum (representing the primary X-rays originating from corona) plus a spectral line (representing the $\text{K}\alpha$ emission line of iron at 6.4 keV rest energy). The line is intrinsically narrow (in the

local co-moving frame) of the line-producing ring, although it becomes subsequently broadened by relativistic effects. The line is produced in a range of radii over the inner disc, so the rings are just those radii where the line production is enhanced above the baseline model of the power-law component and the broad line. The mentioned components of the model spectrum give us an opportunity to test the procedure of reconstructing the source emissivity. Light rays propagate along null geodesics in the curved spacetime, which brings significant energy shifts to the final spectrum and it spreads the observed profile over the whole $\langle g_{\min}, g_{\max} \rangle$ interval with respect to the rest energy of the line.

Figure 1 presents the extremal energy shifts, g_{\max} vs. g_{\min} . These determine the expected energy of the local peaks of the composite broad line, depending on the radial profile of emissivity from the disc. One can see a complex interplay between gravitational effects, Doppler shift and light-bending. The overall gravitational redshift dominates near the horizon (although we restrict the emission radii to $r > r_{\text{ISCO}}$), while Doppler broadens the line (i.e. it increases g_{\max}/g_{\min} ratio) and it enhances the height of blue wing, progressively more for large inclinations. The focusing effect further enhances the observed flux, especially at large i .

Fig. 1 provides several examples including both pro-

¹ In the case of accretion discs counter-rotating with the black hole, we found a disagreement between our energy shifts compared with the corresponding values in Dauser et al. (2010). We checked that the discrepancy up to $\sim 3\%$ (gradually growing with the spin and inclination angle) can be attributed to the way how frame-dragging effects had been treated in the original version of the `relline` code. It turns out that this difference has been meanwhile eliminated from the latest version of the code, so the results are now in full agreement with the `kyrline` (Dovčiak et al. 2004b) version for retrograde spin. Naturally, in the latter case, ISCO can recede as far as $r = 9GM/c^2$, and so the relativistic effects become quite small compared to discs rotating in the prograde direction.

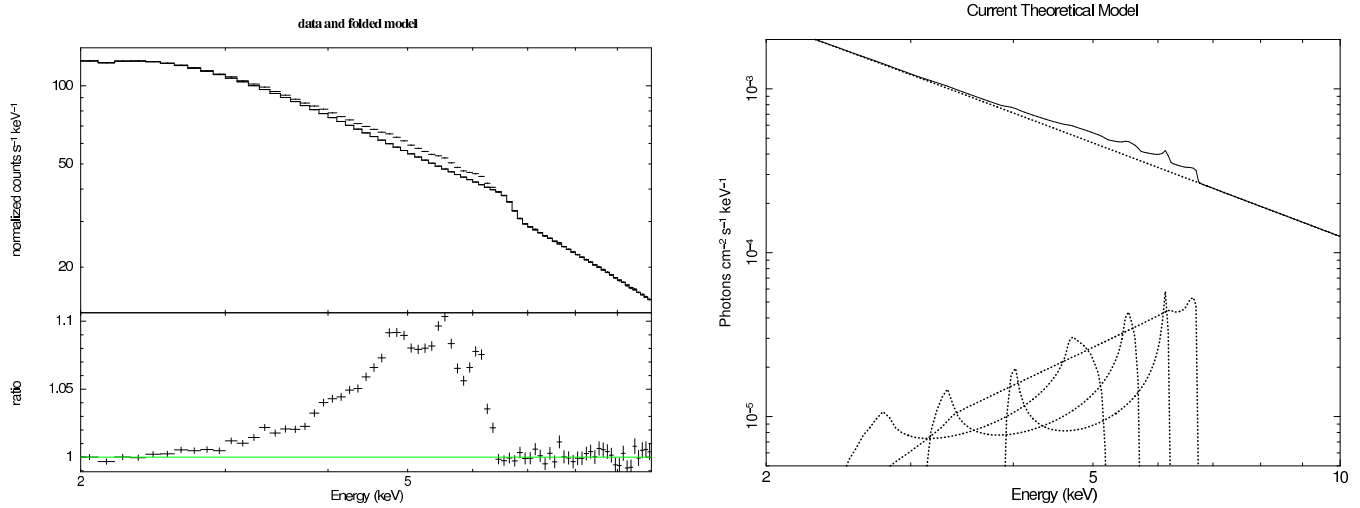


Figure 2. Left panel: Simulated data and the ratio to the the baseline model consisting of the power-law and the disc-line components (background subtracted). Residuals related to the three additional narrow rings are clearly visible. Right panel: The complete theoretical model and the model components: a power-law continuum and the individual line profiles from which the energy shifts of the components are derived.

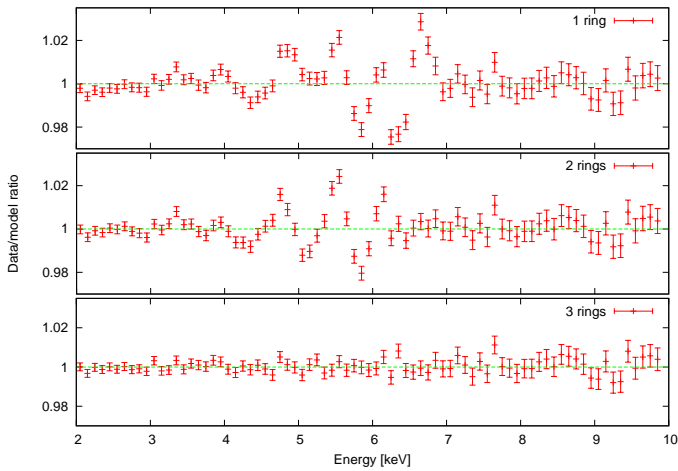


Figure 3. Residuals obtained by fitting the fiducial spectrum by models with a different assumption about the number N of accretion rings. Clearly, $N = 1$ and $N = 2$ cases contain some unmodelled features which allow us to reject these models.

grade and retrograde rotation, although we cannot show here all combinations of the parameters. More examples of the prograde case were examined in Karas & Sochora (2010); in particular; in that work we show also the case of small inclination angles, which are relevant for type-1 AGNs but are more difficult to plot because the energy shifts are much smaller too. From the figure one can also realize that the parameter degeneracy of the model can be expected where the lines converge to each other, quite independent of the parameter values (we will come back to this issue in more detail later in sec. 3).

It is interesting to compare our results with a similar scenario for the geometrical and kinematical properties of the reflection model by Pariev et al. (2001), who also based their discussion on the extreme frequency shifts of a spectral line, as determined by measured radiation fluxes in the iron line wings. In particular, they show contour maps of the

extremal redshift in two limiting cases – a non-rotating ($a = 0$, Schwarzschild) and the maximally co-rotating ($a = M$, Kerr) black hole. Our graphs are given while keeping the view angle i fixed, showing the expected energy of spectral-line wings as the black hole spin is varied (even to negative values).

We note that there is some unavoidable degeneracy among the model parameters. However, we will show that this degeneracy can be avoided in situations where the accretion disc emission is dominated by contributions from a small number of narrow rings located at well-defined radii. Because the gravitational redshift becomes increasingly important as the spin increases and the radius of the ring goes to r_{ISCO} , the rings could be potentially revealed as features on the wing of the underlying relativistically broadened line.

2.3 Test case

The assumed source of reflection spectrum is a set of relatively narrow accretion rings or belts ($\Delta r \sim 0.5r_g$) representing the emission excess above the standard accretion disc spectral line around a rotating (Kerr) black hole. Thanks to the large effective area of the proposed detector (designed to reach $\simeq 12 \text{ m}^2$, i.e. about two orders of magnitude greater than that of XMM-Newton near the iron line rest energy), as well as a sufficient energy resolution about 200–250 eV, the accretion rings should be visible when setting realistic values of the model parameters in our test spectra. For the modelling purposes, as the worst case we assume 300 eV energy resolution.

In order to demonstrate the feasibility of the mentioned scenario we use a preliminary response matrix² as an example of presumed capability of a future large-collecting-area device. This will help us to assess the performance of XMM-Newton versus LOFT and our ability of constraining the model.

² See <http://www.isdc.unige.ch/loft/>.

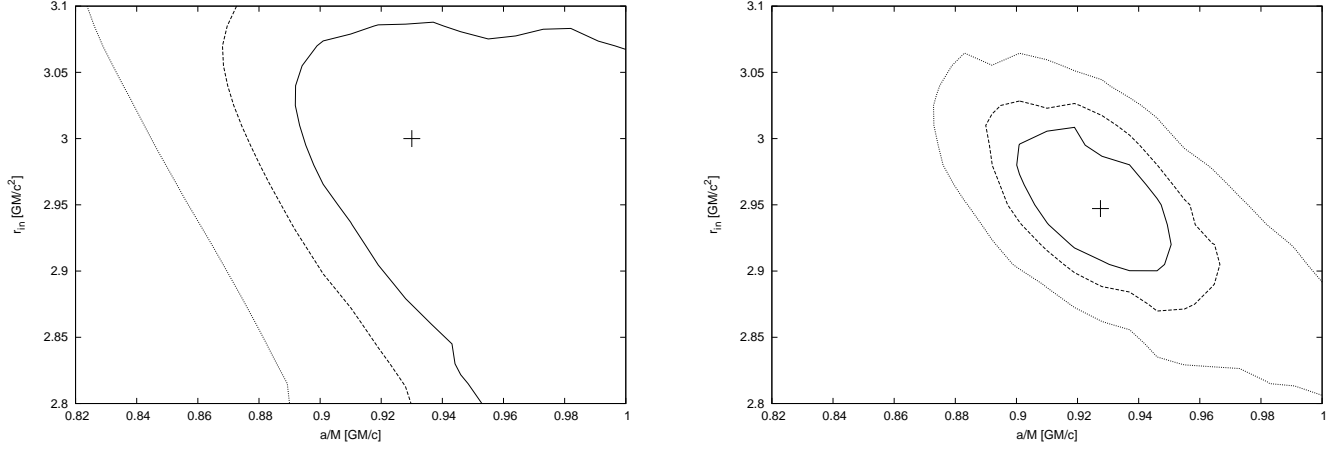


Figure 4. Constraints on the best-fit model parameters are derived from the simulation data. Confidence contours are shown (1, 2, and 3σ) of the inner ring radius r_{in} vs. dimension-less spin a . Left panel: The best-fit case found using the XMM-Newton response matrix with 100 ksec exposure time. Right panel: The same analysis performed with the LOFT preliminary response matrix and 20 ksec exposure.

First, we produced the simulated spectrum by assuming the source flux of approximately 1.3 mCrab ($\simeq 3 \times 10^{-11}$ erg/cm²s in the energy range 2–10 keV), i.e. typical of a nearby bright Seyfert galaxy, such as MCG–6-30-15. We assumed a photo-absorbed power law continuum (photon index $\Gamma = 1.9$, $n_H = 4 \times 10^{21}$ cm⁻²) on top of which the three rings produce a relativistically broadened spectral line (rest energy $E_{\text{rest}} = 6.4$ keV).

We assumed the exposure time of 20 ks for the LOFT mission and compared the model spectrum with the same set-up for 100 ks of XMM-Newton spectrum. It is important to realize that the huge collecting area of LOFT will allow us to constrain the parameters on a significantly shorter observation time, roughly comparable with the orbital time at the corresponding radius. Therefore, the required exposure does not much exceed reasonable duration of the flares, whereas for XMM-Newton it had to be significantly longer.

The configuration of three rings is a reasonable (albeit somewhat arbitrary) trial assumption, where we can test the case of several, but not too many, radially confined excesses in the disc plane. Also the assumed duration of the observation is somewhat arbitrarily set to a value which appears to be reasonably long and realistically achievable at the same time.

We set the ring widths to be initially $0.5r_g$, i.e. comparable with the gravitational radius as a typical length-scale of the system. Other relevant model parameters were set to: $a = 0.93$ (rapidly spinning black hole in prograde rotation), $i = 30^\circ$ (moderate inclination typical of a Seyfert 1 nucleus) as the initializing values. Our fiducial model is therefore `phabs*(powerlaw+4*kyrline)`, i.e. a photo-absorbed power-law continuum and four line components blurred by relativistic effects (we used XSPEC v. 12.6.0). One of the `kyrline` components originates over the entire disc surface and it has been fixed to its defaults parameters ($r_{\text{ISCO}} \leq r \leq 400$, radial emissivity index $\alpha = 3$); it provides the main portion of the total line flux (we set about 60% for definiteness). The other components represent the emission excesses from three ring-type regions, each one giving a smaller fraction ($\simeq 10$ –15%) of the line flux. Naturally, diminishing the line flux produced by the rings relative to the mean flux of the

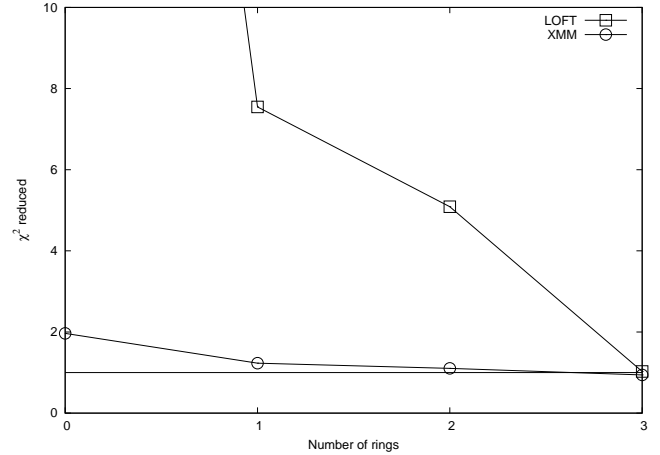


Figure 5. Reduced χ^2 for different best fits to the fiducial model of $N = 3$ number of rings. Three cases are shown: $N = 2$ (two rings), $N = 1$ (one ring), and $N = 0$ (the line component produced only by the disc). Both $N = 1$ and $N = 2$ are statistically acceptable ($\chi^2_{\text{red}} \sim 1$) with the XMM-Newton EPIC-pn response, but they can be excluded by LOFT. The following parameters were thawed for all rings during the fit procedure: a , i , r_{in} , r_{out} . The following parameters were frozen: E_{rest} , Γ , n_H .

entire disc and the powerlaw component makes the determination of g_{max} , g_{min} harder and eventually impossible. We think, however, that the adopted level of the excess emissivity is realistically possible. Figure 2 shows the data to model ratio for the fiducial spectrum. The geometrical location and other parameters of the model components will be now submitted to a standard rigorous fitting procedure.

One expects that a single ring would be easier to recognize in the observed spectrum, while with the growing number of rings and diminishing separation among them the total signal should resemble that of a spectral line smeared over the accretion disc. Can one estimate the model parameters directly, by locating the energy of the peaks in the spectrum?

There is a partial degeneracy of the parameter values.

Ring	g_{\min}	g_{\max}	r_{in}		r_{out}	
			$a = 0.77$	$a = 1.00$	$a = 0.77$	$a = 1.00$
1	0.36	0.81	3.1	2.8	3.7	3.4
2	0.48	0.91	4.1	3.9	4.9	4.7
3	0.59	0.98	5.8	5.6	7.1	6.9

Table 1. Parameters of the model inferred from the energy positions of the spectral peaks in the test spectrum from Fig. 2. We identified the visible features with the horns of the line components. We imposed the same inclination $i = 30$ deg for all three rings and required the inferred spin values to be consistent with each other. The spin turns out to be constrained only partially, with the values from 0.77 up to 1.00 being consistent with the positions of peaks in the model spectrum when the radius is set appropriately. The fiducial test spectrum was generated for rings position at radii $r_{\text{in}} = 3r_g$, $4r_g$, and $6r_g$, respectively. The tabulated values demonstrate the accuracy of the fitting procedure. See the text for details.

In our case this exhibits itself by the fact that, in order to obtain the red peaks of the line in right positions, the spin has to be greater than the lower limit of $a = 0.77$, however, the upper bound remains undetermined (up to $a = 1$). For $0.77 \leq a \leq 1$, i.e. up to the maximum spin of the Kerr black hole, we can reproduce the peaks by rearranging the ring radii. This is shown in the table by giving two possible values of r_{in} and r_{out} that are consistent simultaneously with the mention minimum and maximum values of spin. One can see that the uncertainty in the inferred radii is below 10%, while for spin the relative error represents about 25%.

Although the “visual” approach to infer the peaks of the line profile constrains the model quite well, it does not allow us to determine the errors and to perform the formal statistical confidence contours analysis, so that apparently accurate values of g_{\max} and g_{\min} cannot be assigned a proper meaning. The spectral fitting should result in a more reliable determination of the parameters because it employs the whole spectral shape. This appears to be important especially in the situation when the large effective area allows to resolve the broad line. On the other hand, the spectral fitting tends to be sensitive to the assumed spectral model. In order to clarify the situation we carry out the following test.

We subjected the fiducial model to the standard XSPEC fitting procedure with the aim of recovering the initial model parameters including their confidence contours. In particular, we tested if the assumed number of rings can be recovered with a significant confidence. In figure 3 we show the best-fit residuals with respect to the continuum model, i.e., the plot was obtained by removing the `kyrline` component from the best-fit spectra (we show unbinned data because any definitive information about the future detector the quoted energy resolution is still preliminary at present). The number of rings was changed from the original $N = 3$ to $N = 2$ and $N = 1$. As free parameters we re-fitted the spin a , inclination i , and the radial width of rings, Δr . The rest energy of the line was fixed (it was allowed to vary in subsequent tests). The position of the rings can be also allowed to change, although the procedure cannot start too far from correct values because of local minima in the χ^2 space.

By setting the number of rings to the fiducial number we recover correctly the initial values of the parameters as expected, while different numbers of rings produce worse fits and the parameters converging off the right values (or not converging at all). We examined also the case of the line

emission spread over the entire disc surface (this represents the standard disc-line model), but the resulting fit was bad.

In order to compare the results expected from LOFT with those that can be reached with currently available data, we carried out the same procedure as described above also with the XMM-Newton response file of the EPIC-pn camera. Figure 4 demonstrates the expected accuracy with which the model parameters are constrained. We plot the confidence contours for the inner ring radius versus the black hole spin. With the same exposure and the source brightness for both instruments, LOFT will allow us to set much tighter constraints on the best-fit values.

In figure 5 we show the resulting best-fit χ_{red}^2 values. Decreasing the number of rings from the right value $N = 3$ obviously degrades goodness of the fit. For XMM-Newton the best-fit χ_{red}^2 values are lower, meaning that the model parameters are constrained at deteriorated confidence compared to LOFT. Both $N = 1$ and $N = 2$ tests give (wrongly) acceptable fits for XMM-Newton, while they can be clearly rejected with LOFT. Naturally, $N = 3$ gives a good fit because our artificial data were created with this value, so we only reproduce the original input. Increasing the number of rings above $N = 3$ produces formally acceptable statistics, but the number of model parameters then exceeds the necessary minimum. This indicates an encouraging improvement that could be achieved for this particular problem with the improved sensitivity of LOFT.

3 DISCUSSION

Parameter constraints could be improved also in our test case of XMM-Newton, if the observation duration can be made longer and the number of collected photons correspondingly larger. Because in practice one cannot prolong the duration above some reasonable limit, the increase of the collecting area of the LOFT detector is the most important aspect which improves the parameter constraints. The energy resolution of the detector is a less critical factor because the effect of relativistic broadening causes the line width to be much broader than this limit by a significant margin.

We remark that the special choice of $N = 3$ was needed for illustration purposes described above, but it does not mean any crucial limitation that would be essential for the described idea or the method. Naturally, a lower number of rings is easier to be recognized in the spectrum and its parameters to be reconstructed correctly. On the other hand, in the case of large N the magnitude of the re-

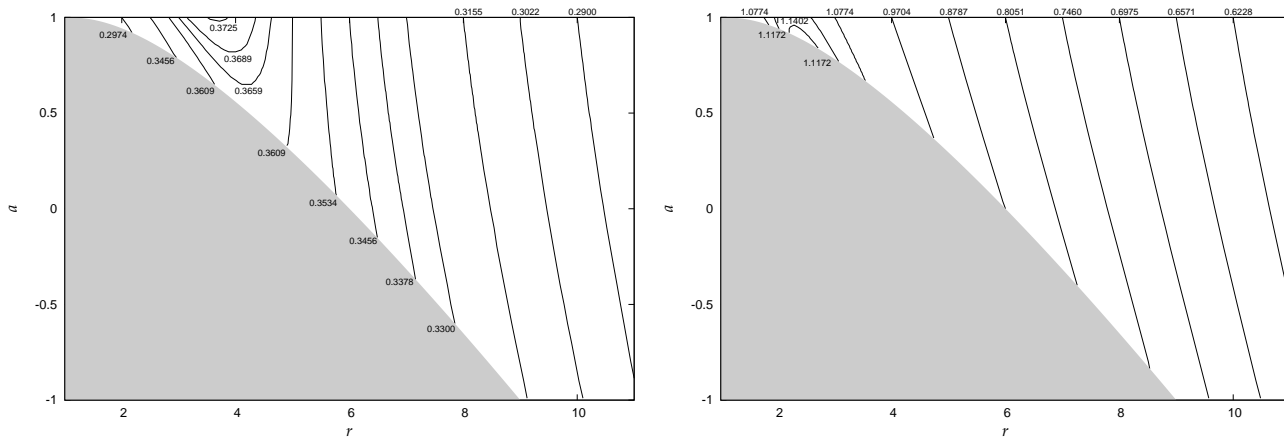


Figure 6. Contours of the energy difference $\delta g(r, a; i)$ of the Doppler peaks of the observed spectral line profile, as a function of the dimensionless radius r (units of GM/c^2) of the ring and the spin a of the black hole. $\delta g(r, a; i)$ defines the factor of relativistic broadening of the line. Left panel: view angle $i = 30$ deg; right panel: $i = 75$ deg. Although the role of spin generally increases as the distance gets smaller, we notice that $\delta g(r, a; i)$ becomes insensitive to a at a certain distance. The shaded area represents the region below ISCO.

sulting peaks above the baseline profile becomes relatively small and the situation turns into the problem discussed by Wilkins & Fabian (2011), i.e. the disc-line emission imagined as consisting of infinitesimal rings extending all the way from the inner to the outer rim of the disc.

We asked ourselves whether the energy position of the observed peaks determines the system parameters r , i , and a in any unique way, or if instead the proposed procedure of reconstructing the parameter values converges to several different results, depending on the initial guess of the parameter values. In fact, the latter is true. Therefore we need to set addition constraints in order to help XSPEC to find the right answer. We can demonstrate this complication in another way, by plotting the observed energy difference $\delta g(r, a; i)$ of the line peaks in figure 6: $\delta g \equiv g_{\max} - g_{\min}$. Notice that the dependence of δg on spin is ambiguous in some parts of the parameter space.

In some situations – namely, for small radii and large spins – the energy separation of the two peaks the observed profile is not in one-to-one correspondence to model parameters; it is instead a double-valued quantity with respect to a (as can be seen in the top left corner of the fig. 6 left panel). Naturally, at large radii and small inclinations the spin dependence on δg is weak, and so the practical use of the method becomes compromised. On the other hand, we do see the range of the parameter space (typically for radii between $r \simeq 4$ and $\simeq 12$), where the spin dependence is non-negligible and the possibility of reconstructing the parameters appears quite promising. We can also notice an interesting conspiracy when the contour-line takes almost straight vertical direction (e.g. in the same plot for $i \simeq 30$ deg, $r \simeq 5GM/c^2$), implying that spin is degenerate with respect to radius for that given inclination.

Also, a narrow Fe line – so ubiquitous in the X-ray spectra of type-1 AGN – will be unresolved by LOFT due to the poor energy resolution of its Large Area Detector (LAD). This could lead to confusion with the blue wing of the relativistic line if it happens to come close to the rest energy of the neutral line. However, it does not mean an unsurmountable complication because these narrow fea-

tures are thought to originate via scattering by a distant reflector (e.g. a torus of matter located at several thousand gravitational radii, or more). Therefore, the narrow component does not vary on short time-scales and its influence can be taken into account by estimating the flux from other, high-energy resolution spectroscopy, and including it in the model. Indeed, most of candidate objects for a relativistic line were already observed by XMM-Newton (Nandra et al. 2007; de la Calle Pérez et al. 2010), although a concurrent detection by LOFT together with another high-energy resolution mission would be the best strategy.

Naturally, the problem of confusion or non-uniqueness would appear if the broad line is produced farther out from ISCO (several tens of r_g and more), so that the observed width is only moderate and comparable with the detector intrinsic energy resolution; for such cases the LOFT will not be suitable. We remark that the aforementioned simulations were performed for the response matrix resolution of 300 eV. It is currently expected that a better resolution of about 200–250 eV can be realistically achieved (Feroci et al. 2011), and so the obtained constraints should come out as even more favourable compared to the results presented here. As an example, we constructed the confidence contours of Fig. 4, but with the energy resolution of 180 eV (an optimistic expectation), and we checked that the contour levels come out very similar to those shown for 300 eV resolution in the right panel. Both sets of best-fit values are consistent with each other.

The above-given simulations suggest that the mentioned features should be detectable around the iron line rest energy in bright accreting supermassive black holes. The foreseen energy resolution of the detector is sufficient to reveal moderately broad excesses emerging on top of the underlying continuum (unless the resolution becomes significantly worse than the currently discussed value about 200 eV). The signal-to-noise level would be more of a concern especially if the background level were not determined with sufficient confidence. Our example demonstrates that bright AGNs (such as MCG-6-30-15 during a prominent flare of Ponti et al. 2004) should be accessible to this kind of study.

To this end, the background model is required to be stable to approximately 5% accuracy.³

The expected signal from AGNs will be background dominated with LOFT. Therefore, for the applications discussed in this paper, the precise determination of the background model is important, especially near the iron line rest energy. More detailed studies of the background impact are needed, however, currently available estimations (Feroci et al. 2011) suggest sufficient stability of the background model on the time-scales exceeding the orbital periods in the inner regions of AGN accretion discs. Promising targets can be picked up from the list by de Marco et al. (2009, and further references cited therein); these objects have already exhibited the presence of transient narrow-line features that could be relevant for our study.

Naturally, Galactic black holes in X-ray binaries represent another category of potential targets, assuming one can identify a suitable source with the flare-induced reflection signatures, similar to those seen in AGNs. According to the current specifications, the temporal resolution does not pose serious limitations (thanks to the large collecting area and sufficiently fast response time), even though the characteristic time-scale decreases proportionally to the mass, i.e., by 6–7 orders of magnitude shorter for Galactic black holes compared to supermassive black holes. On the other hand, high ionisation levels are typical of Galactic black holes, and these may prevent successful detections despite the favorable source brightness that exceeds typical AGNs.

The adopted scenario has clearly an interesting potential to discriminate between the reflection model of spectral features from the case when the obscuration by intervening material and the resulting absorption are the main agents modulating the power-law continuum and shaping the observed spectrum.

In summary, we arrive at the conclusion that the fiducial values of the model parameters can be reconstructed with the anticipated capabilities of LOFT. Although in this paper we considered the spectral features formed by azimuth-integrated rings, our preferred scenario of forming these rings is by orbital motion of spatially localized flares. We note that the LOFT mission is dedicated primarily to timing studies. Indeed, it should provide us with light curves of flares to much better time resolution than any of its predecessors. Temporal profiles of the flare onset and the subsequent decay exhibit some signatures of model parameters (see fig. 7 in Goosmann et al. 2007), but these are beyond current observational capabilities. Once resolved, they will give us a complementary information that can be compared against spectral studies discussed in the paper.

4 CONCLUSIONS

We explored a possibility of studying relatively indistinct excesses on top of the relativistically broadened spectral line

profile. Unlike the main body of the broad line, thought to originate from a whole extended region of the accretion disc, we modelled these features as the emission-line components arising in well-confined radial distance in the accretion disc. We also suggested that some energetically narrow features could be explained as a signature of spatially localized irradiation by magnetic reconnection flares above the underlying accretion disc. Because of prevailing rotational motion of the accreted material and unavoidably prolonged duration of observations necessary to collect enough photons, even such localized events should reveal themselves in the observed spectrum as emission rings.

We found that the presence of about 10–15% excess emission of the line flux originating from a ring of a moderate width (typically a fraction of gravitational radius) close to the black hole could be tested by the proposed LOFT satellite. The effective area of this mission is designed to be large enough to allow the model parameters to be constrained despite its limited energy resolution. This will significantly reduce the degeneracy of the model parameters – a notorious obstacle complicating interpretations of the current data. One needs to note that the ability of converging to the correct parameter values could be compromised if the background level is significantly increased above our default estimation, so this issue will need further investigation. In fact, bright Galactic stellar-mass black-hole candidates may be more suitable sources, as AGN will be always dominated by the background.

In this paper we concentrated ourselves to the supermassive black hole especially because in this case the baseline model can be assumed in a relatively simple form and the iron-line complex has been commonly detected in AGN, nevertheless, bright Galactic binaries with accurately modelled spectral components may be eventually a more suitable category of targets. At this stage we could only verify that the anticipated background level does not pose a serious limitation for the example described above, assuming that the background model is itself known with the sufficient accuracy. This issue will need further investigation especially because the background level is expected to vary with energy, and so, in principle, inaccuracy of the background model could arise.

A typical double-horn profile gives us an opportunity to determine the parameters by measuring the energy shifts of the features within the broad spectral line wings. The observed energy of these features is well-defined (assuming a sufficiently narrow radial extent of the rings). Naturally, the inferred parameters from different rings should be consistent with each other (e.g. the same inclination, assuming that the rings reside in the same equatorial plane). This will help us to distinguish the disc-line geometry of the line emitting region from alternative options, such as the lines originating in outflows and jets (Wang et al. 2000), spiral waves (Hartnoll & Blackmann 2002), or geometrically thick non-Keplerian tori (Fuerst & Wu 2007).

Even in situations when the contribution of rings is only moderate and the energy shifts cannot be determined immediately from the secondary peaks merely by inspecting the spectrum, the fitting procedure can be employed to reconstruct the model parameters. This requires employing a physically substantiated model of the spectrum and using the entire profile of the broad line and the continuum. Nat-

³ We tested the expected impact of background contamination by applying `corrnorm` to the background file in XSPEC. Randomizing the background at 3, 5, and 10% levels, respectively, we checked that the parameters of our fiducial model are well-reproduced in the first two cases, while the 10% inaccuracy of the background would seriously degrade the best fit constraints.

urally, in the latter case the assumptions about the intrinsic spectrum are essential.

The concept seems to be well suited to study the effects which are often coined as “strong gravity” in the astrophysical context. Despite a limited energy resolution and various convergence issues of the spectral fitting procedure discussed in the paper above, the large effective area offers a significant progress over what can be presently achieved with XMM-Newton not only in the case of timing studies but also for the spectroscopy of truly broad relativistic spectral features.

ACKNOWLEDGMENTS

We thank Dr. Alessandra de Rosa for advice concerning the background estimation, and an unknown referee for useful comments. This research is supported by the ESA PECS project No. 98040. VK and MD gratefully acknowledge support from the Czech Science Foundation grant 205/07/0052 and the Ministry of Education project ME09036. VS is supported by the doctoral grant GAČR No. 205/09/H033. JS acknowledges support from the grant GAČR 202/09/0772. Part of this work has been carried out within the COST Action MP0905 – Black Holes in a Violent Universe.

REFERENCES

- Abramowicz M. A., Jaroszyński M., Kato S., Lasota, J.-P., Różańska A., Sadowski A. (2010), *A&A*, 521, A15
- Artymowicz P., Lin D. N. C., Wampler E. J. (1993), *ApJ*, 409, 592
- Ballantyne D. R., McDuffie J. R., Rusin J. S. (2011), *ApJ*, 734, id. 112
- Coppi B., Rousseau F. (2006), *ApJ*, 641, 458
- Cuadra J., Armitage P. J., Alexander R. D., Begelman M. C. (2009), *MNRAS*, 393, 1423
- Czerny B., Różańska A., Dovčiak M., Karas V., Dumont A.-M. (2004), *A&A*, 420, 1
- Dauser T., Wilms J., Reynolds C. S., Brenneman L. W. (2010), *MNRAS*, 409, 1534
- de La Calle Pérez I., Longinotti A. L., Guainazzi M., Bianchi S., Dovčiak M. et al. (2010), *A&A*, 524, A50
- de Marco B., Iwasawa K., Cappi M., Dadina M., Tombesi F. et al. (2009), *A&A*, 507, 159
- Dovčiak M., Bianchi S., Guainazzi M., Karas V., Matt G. (2004a), *MNRAS*, 350, 745
- Dovčiak M., Karas V., Yaqoob T. (2004b), *ApJS*, 153, 205
- Fabian A. C., Iwasawa K., Reynolds C. S., Young, A. J. (2000), *PASP*, 112, 1145
- Fabian A. C., Pounds K. A., Blandford R. D. (2004), *Frontiers of X-Ray Astronomy* (Cambridge University Press: Cambridge)
- Feroci M., Stella L., Vacchi A., Labanti C., Rapisarda M. et al. (2010), *Proc. SPIE*, 7732-66 (arXiv:1008.1009)
- Feroci M., and the LOFT Consortium (2011), *Experimental Astronomy*, in press
- Fuerst S. W., Wu Kinwah (2007), *A&A*, 474, 55
- Goosmann R. W., Mouchet M., Czerny B., Dovčiak M., Karas V., Różańska A., Dumont A.-M. (2007), *A&A*, 475, 155
- Guainazzi M. (2003), *A&A*, 401, 903
- Hartnoll S. A., Blackmann E. G. (2001), *MNRAS*, 332, L1
- Kato S., Fukue J., Mineshige S. (1998), *Black-hole Accretion Disks* (Kyoto University Press: Kyoto)
- Karas V., Martocchia A., Šubr L. (2001), *PASJ*, 53, 189
- Karas V., Sochora V. (2010), *ApJ*, 725, 1507
- Karas V., Šubr L. (2001), *A&A*, 376, 686
- King A. R., Pringle J. E. (2006), *MNRAS*, 373, L90
- Markowitz A. G., Reeves J. N. (2009), *ApJ*, 705, 496
- McClintock J. E., Remillard R. A. (2006), In: *Compact Stellar X-ray Sources*, eds. W. Lewin & M. van der Klis (Cambridge: Cambridge University Press), pp. 157–213
- Miller J. M., Fabian A. C., Wijnands R., Remillard R. A., Wojdowski P. et al. (2002), *ApJ*, 578, 348
- Nandra K., O’Neill P. M., George I. M., Reeves J. N. (2007), *MNRAS*, 382, 194
- Novikov I. D., Thorne K. S. (1973), in *Black Holes*, eds. C. DeWitt and B. S. DeWitt (New York: Gordon and Breach Publishers), p. 343
- Page D. N., Thorne K. S. (1974), *ApJ*, 499, 191
- Pariev V. I., Bromley B. C., Miller W. A. (2001), *ApJ*, 547, 649
- Ponti G., Cappi M., Dadina M., Malaguti G. (2004), *A&A*, 417, 451
- Reynolds C. S., Fabian A. C. (2008), *ApJ*, 675, 1048
- Reynolds, C. S., Nowak, M. A. (2003), *Phys. Rep.*, 377, 389
- Schnittman J., Krolik J. H., Hawley J. F. (2006), *ApJ*, 651, 1031
- Svoboda J., Dovčiak M., Goosmann R., Karas V. (2009), *A&A*, 507, 1
- Svoboda J., Guainazzi M., Karas V. (2010), *A&A*, 512, A62
- Tagger P., Varnière P. (2006), *ApJ*, 652, 1457
- Uzdensky D. A., Goodman J. (2008), *ApJ*, 682, 608
- Wang J.-M., Zhou Y.-Y., Yuan Y.-F., Cao X., Wu M. (2000), *ApJ*, 544, 381
- Wilkins D. R., Fabian A. C. (2011), *MNRAS*, 414, 1269